Two-dimensional percolation and cluster structure of the random packing of binary disks

D. He,* N. N. Ekere,* and L. Cai*
School of Aeronautical, Civil, and Mechanical Engineering, The University of Salford, Salford M5 4WT, United Kingdom
(Received 22 October 2001; published 25 June 2002)

In this paper we study the short-range correlated percolation and the cluster structure of two-dimensional (2D) random packing of binary disks with size ratio λ in the range of 1–5. A Monte Carlo simulation model is used to generate the configuration of random packing first. Then a from-neighbor-to-neighbor propagation method is used to identify the number and sizes of the clusters. Results show that for $\lambda=1$ the percolation threshold p_c lies between the square and triangular site percolation thresholds. As λ increases the percolation threshold p_c (the area fraction of small disks) decreases. To characterize the cluster structure at the percolation threshold, we scale the cluster size s_c with the cluster radius R as $s_c \propto R^D$. The fractal dimension D obtained lies between 1.86 and 1.88 and is independent of the size ratio λ. This value is in good agreement with the 2D theoretical fractal dimension which is equal to 91/48.

DOI: 10.1103/PhysRevE.65.061304 PACS number(s): 45.05.+x, 64.60.Ak, 05.70.Jk, 05.10.Ln

I. INTRODUCTION

The short-range correlated percolation process has been extensively studied for more than half a century. This is due to its effectiveness in solving problems in disordered systems in a variety of scientific and engineering fields, such as the fluid flow in porous media, the forest fire spread, and the transportation network [1,2]. Perhaps the most important application of the percolation process is in the study of the physical properties and the phase transition of composite materials [3–8]. A straightforward example is a binary composite composed of electrical conductive elements and insulating elements. As the volume fraction p of the conductive elements is lower than a critical value the composite behaves as an insulator. As p approaches a critical value p_c the composite experiences an insulating-to-conducting phase transition. This is attributed to the formation of a cluster of the conductive elements that spans the composite. The critical value p_c is referred to as the percolation threshold.

Monte Carlo simulation technique is a powerful tool in solving the percolation problem and many simulation models have been developed [9–14]. In classical site percolation models, each site of an ordered lattice, e.g., square, honeycomb, or triangle in two dimensions (2D), and diamond or simple cubic in 3D, is randomly occupied by a conductive particle with probability p or by an insulating particle with probability $1-p$. The main aim of the simulation is to find the percolation threshold p_c, the lowest volume fraction of the conductive particles, at which the largest cluster of the conductive particles spans the entire simulation domain. For 2D square lattice site percolation it has been obtained by many that p_c is about 0.593, and for triangular lattice $p_c = 0.50$ [1,2,12]. At percolation threshold p_c the cluster structure can be characterized by several geometrical parameters, such as the cluster size and number, the cluster radius, and the correlation length. Near the percolation threshold p_c some of the physical properties of a composite will obey the universal law $\Psi \propto (p-p_c)^\beta$, where Ψ represents a physical property, such as the conductivity. The exponent β is insensitive to the microstructure of the composite.

The above description implies that two assumptions are made in the classical percolation model. The first one is the ordered lattice, which means the positions of the particles are preknown, and what is not known is which particles are conductive. The second one is that all the particles have the same size. In practice, however, there are many disordered systems in which both the positions and sizes of the particles are randomly distributed, such as the amorphous composites and the compacts with two or more types of granular powders. It has been found for many years that, in a compact of the mixture of metallic powder and polymeric powder, lower electrical conductive percolation threshold p_c (here p_c is the volume fraction of metallic powder) can be obtained by increasing the particle size ratio λ of the polymeric powder to the metallic powder [15–17]. Understanding the effect of λ on p_c will allow material scientists to optimize the physical properties by adjusting the compositions of the materials, such as conductive polymer [18], adhesives [19], and ceramics [20]. A few analytical models have been developed to predict the effect of λ on the percolation threshold p_c of the compacts with binary particles [15,17,21,22]. In the model developed by Malliaris and Turner [15] it is assumed that each large polymeric particle is covered by a monolayer of metallic particles. The percolation threshold predicted by this model is significantly lower than that obtained by experiments. The other models are modifications of this model. A common assumption made in these models is the segregated distribution of the metallic particles, which means that the small metallic particles are only distributed in the neighborhood regions of the surfaces of the large polymeric particles. Therefore, these models are only valid under the condition $\lambda \gg 1$. Another shortcoming is that these models cannot provide the structure information in detail. Even with a high value of λ, aggregates of fine particles have been observed in the conductive adhesive [19]. Thus we may conjecture that, in the compact of binary particles, if λ is not too far from one, both large and small particles should be randomly distributed without bias. The percolation problem of such systems has been rarely reported in the literature.

*Present address: Medway School of Engineering, University of Greenwich at Medway, Chatham Maritime, Kent ME4 4TB, U.K.

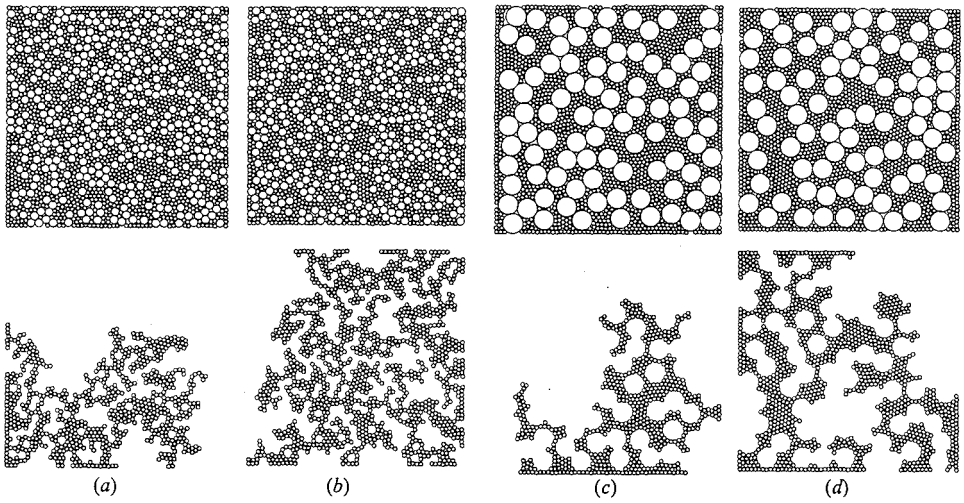

FIG. 1. Random packings and the largest clusters $s_{\max}$: (a) $\lambda=2$, $n=2000$ $p=0.480$, $s_{\max}=731$; (b) $\lambda=2$, $n=2000$, $p=0.499$, $s_{\max}=1286$; (c) $\lambda=5$, $n=1500$, $p=0.391$, $s_{\max}=609$; (d) $\lambda=5$, $n=1500$, $p=0.412$, $s_{c,\max}=1103$.

We have developed a Monte Carlo simulation model that can be applied to investigate the percolation process of 2D and 3D random packing of binary particles and to characterize the cluster structure at the percolation threshold p_c. This model completely differs from the continuum percolation models [23–26] in which particles are allowed to overlap each other to form percolating clusters. In Sec. II we introduce the simulation technique; in Sec. III we present 2D simulation results and discussion; and finally we summarize the conclusion of this study.

II. THE SIMULATION MODEL

The simulation model is composed of two parts. The first part is the generation of a 2D random packing of disks, and the second part is the identification of clusters. For convenience, we assign the diameter of the small disks to be one unit; then the diameter of large disks equals the size ratio λ. The area fraction p of small disks is given by

$$p=\frac{n_s}{n_s+n_l\lambda^2}, \tag{1}$$

where n_s is the number of small disks, and n_l is the number of large disks. The total number of disks $n=n_s+n_l$. As $\lambda=1$, the definition of p is identical with that of the classical site percolation models, which is the ratio of the occupied sites to the total sites. Thus we can compare the result of random packing with the result of ordered lattice packing. To avoid confusion, it is necessary to point out that this definition is different from that of the continuum percolation model, which is the ratio of the area of the total disks to the area covered by the disks.

For given values of p, λ, and the total number of disks n, we randomly assign n_s, which is an integer nearest to $np\lambda^2/(1+p\lambda^2-p)$ obtained from Eq. (1), small disks and $n-n_s$ large disks. The initial positions of the disks within a square with initial area of L^2 are also randomly generated that obey uniform distribution. The simulation is started with a very high packing density

$$\Phi=\frac{\pi(n_s+n_l\lambda^2)}{4L^2}. \tag{2}$$

thus there are many overlaps among the disks. Then a relaxation iteration is applied to reduce or eliminate the overlaps. After the relaxation iteration the disks are more uniformly distributed, and the mean overlap reduces to a stable value. According to the mean overlap value, the packing area L^2 is expanded, which leads to the decrease in the packing density Φ. By repeating the relaxation and expansion procedures we can finally obtain the overlap-free packing. Figure 1 shows a few final configurations of the random packings with different values of p and λ. In Fig. 1 each configuration only involves 1500 or 2000 disks, which is only for the convenience of observation. Readers interested in details of the random packing model are referred to Ref. [27]. Statistic tests show that, for $\lambda>1$, the packing is random, homogeneous, and isotropic although triangular orders exist in the scale of a few disk diameters that can be observed in Fig. 1. For $\lambda=1$, previous studies showed that the random packing density Φ falls in the range of 0.82–0.89 [28], and that as the packing density increases the equal disks intrinsically tend to the triangular orders; thus polycrystalline structures are more likely to be attained than completely random structures [29]. The packing density we obtained is $\Phi=0.865$, which is significantly higher than the square packing density $\Phi=0.785$ and lower than the triangular packing density $\Phi=0.907$. In the packing we also found that about 46% of the disks have six nearest neighbors (the nearest neighbor number of triangular packing) compared with that only less than 13% in the random packing with $\lambda>1$. Therefore, it is suitable to classify the packing we obtained for $\lambda=1$ to polycrystalline structure.

Two steps are involved in the identification of the clusters. The first step is to count the nearest neighbors for each disk. To do this we examine the center-to-center distance between any two disks of the same type to detect if they touch each other. In the second step starting from an arbitrary seed disk we count its neighbors and put them in a seed list; then we sequentially take the disks from the seed list and count their neighbors, which are put in a new seed list. A disk may (and

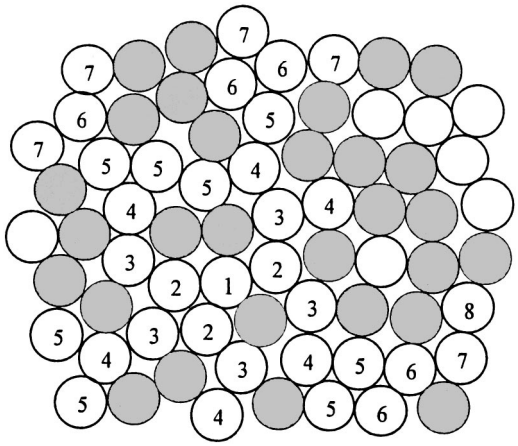

FIG. 2. Sketch of identification of clusters.

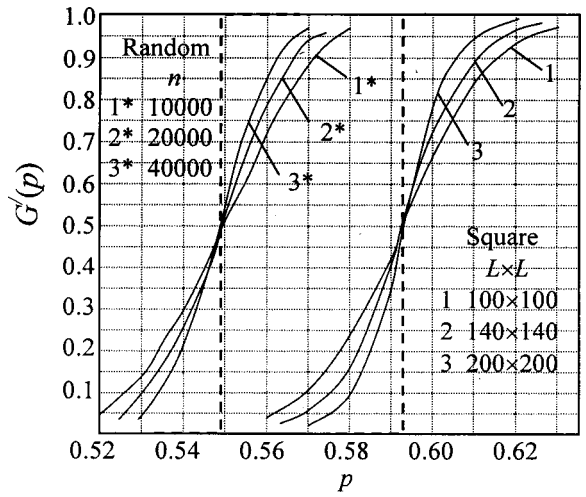

FIG. 3. Effect of system size of $G'(p)$ (equal disks).

often) belong to the nearest neighbors of two or more seeds, and two seeds may also be of the nearest neighbors to each other. Thus to avoid any disk to be repeatedly counted, after counting each disk for the first time we label it, and afterward we only count the unlabeled disks. By this from-neighbor-to-neighbor propagation we can identify all the disks belonging to the same cluster. This process is sketched in Fig. 2 in which $\lambda=1$. The white and dark circles represent the two types of disks, respectively, and we are concerned with the white circles only. The disk marked by 1 represented the first seed, those marked by 2 are the nearest neighbors of the first seed, and their nearest neighbors are marked by 3 and so on. By this process one can see that any disk marked by $i+1$ is approached from one of those marked by i. One can also see that any disk belonging to this cluster can be counted and only counted once because we have labeled it after it was counted for the first time. As all the disks belonging to the same cluster have been counted, we have the size of this cluster $s=1+n_2+n_3+\cdots+n_m$, where n_i is number of disks marked by i in Fig. 2. After finishing the counting of one cluster we start from an arbitrary unlabeled disk (the unmarked white circles in Fig. 2) to count the size of another new cluster by the same process described above. Finally we can obtain the total number of clusters and their sizes in the random packing. Figure 1 also shows the largest clusters corresponding to the random packings. For each cluster we simply examine its horizontal and vertical spanning distances to identify if it percolates the space covered by the disks in either one or in both directions.

III. RESULTS AND DISCUSSION

Applying the above Mont Carlo model we investigated the effect of λ on the percolation threshold p_c and the structural properties of the clusters at p_c of the random packing.

A. The percolation threshold

For $\lambda=1$, we generated three configurations with 10 000, 20 000, and 40 000 disks. The aim of using different number of disks is to examine the potential effect of the finite system sizes. For each configuration at a given value of p we took 500 samples and counted the percentage $G'(p)$ of those in which there exist percolating clusters. The values of $G'(p)$ in vertical direction and in horizontal direction were counted, respectively, and them averaged. For $\lambda>1$, at each value of p we generated 40 configurations each involving 20 000 disks. Then we identified the cluster number and sizes in each configuration, and counted the percentage $G'(p)$. In our simulation the increment in p was 0.005, which allows reasonably accurate estimation of the percolation threshold.

For finite-size systems at given occupancy p the probability $G(p)$ of the existence of percolating cluster has been reported in several investigations [30–32], which suggest that at the percolation threshold p_c, in a given direction the probability $G(p_c)\rightarrow 0.5$ as $L\rightarrow\infty$. Lee and Torquato studied 2D continuum percolation of uniform disks with rigid cores and penetrable shells, and their result also implicates that as $L>7$ $G(p_c)$ approaches 0.5 (see Fig. 3 in [33]). Thus we may conjecture that $G(p_c)$ is independent of the packing lattices. To verify the conjecture, we also simulated the site percolation of square lattices with sizes of 100×100, 140×140, and 200×200. At each value of p we took 500 samples. Figure 3 shows the results of square lattice packings and random packings of equal disks. It is seen that for square lattices the curves nearly cross at the same point at which $G'(p)$ is about 0.5 and p is about 0.593, which is the site percolation threshold p_c. For the random packings of equal disks the trend similar to that of the square lattice can also be observed, that is at p just below 0.55 the values of $G'(p)$ with different sizes all approach 0.5. This supports the conjecture that it is independent of the packing lattice that, at the percolation threshold $p_cG'(p)$, approaches 0.5. We may also conjecture that this relationship is applicable to the systems with $\lambda\neq1$. Thus, corresponding to $G'(p)=0.5$ we can estimate the percolation threshold p_c as shown in Fig. 4.

Zallen [34] suggested that in the random packing of equal spheres (disks in 2D), as the packing density Φ and the mean nearest neighbor number z increase the percolation threshold p_c decreases. For $\lambda=1$, we know that for square packing $\Phi=0.785$, $z=4$, and $p_c=0.593$; and for triangular packing $\Phi=0.907$, $z=6$, and $p_c=0.500$. The packing density and the

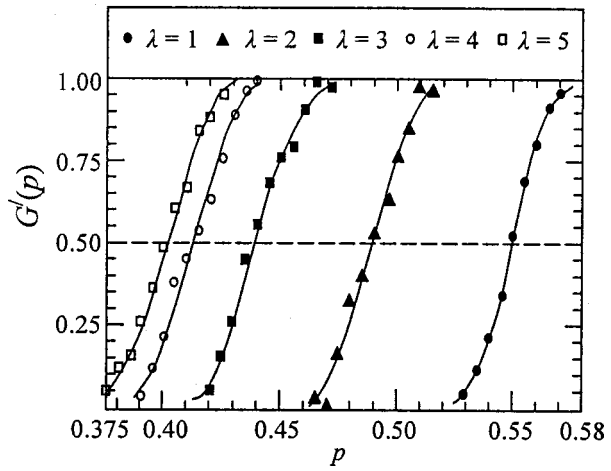

FIG. 4. Effects of λ and p on $G'(p)$.

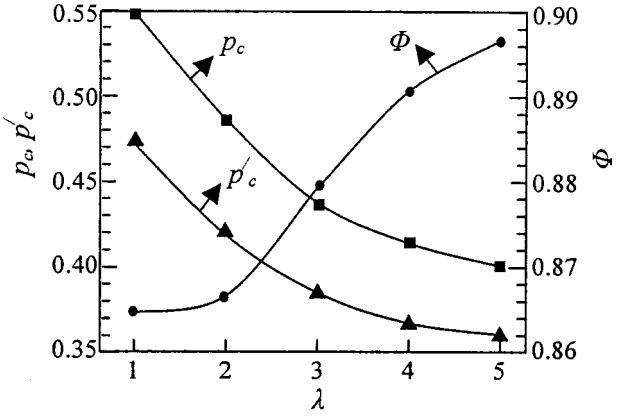

FIG. 5. Effects of λ on the packing density Φ, and on the percolation thresholds p_c and p_c'.

mean nearest neighbor number we obtained for $\lambda=1$ are $\Phi=0.865$ and $z=4.87$, respectively, both lying between that of the square and the triangular packings. Therefore, the percolation threshold should also lie between that of the square and triangular packings. The above argument suggests that the percolation threshold $p_c=0.550\pm0.005$ for random packing is reasonable.

From Fig. 4 we can observe that the percolation threshold p_c decreases with the increase in λ. Table I lists the values of p_c corresponding to the values of λ. The effect of λ on p_c obtained by this random packing model is in qualitative agreement with that of the 3D segregation models [15,17,21,22]. We also observe that near $\lambda=1$, the effect of the increase in λ on p_c is more significant than that as λ is far from 1. For example, as λ increases from 1 to 2, the decrease in p_c is about 0.065; while as λ increases from 4 to 5, the decrease in p_c is only about 0.013. A reasonable explanation may be given by the following argument. In a random packing of binary disks, we may expect that the larger the sum of the perimeters of the small disks the higher the probability for the small disks to form a percolating cluster. With the same area of small disks and large disks that is $n_s\pi/4=n_l\pi\lambda^2/4$, the sum perimeters of the small disks and the large disks are $n_s\pi$ and $n_l\pi\lambda$, respectively, from which we get the ratio of the sum perimeters of small disks to large disks to be λ. Thus, first we see that the ratio of the sum perimeters of small disks to large disks increases with λ, which leads to the decrease in the percolation threshold p_c of the small disks. Second, as the size ratio increases from λ to $\lambda+1$, the relative increase in the perimeter ratio is $1/\lambda$, which becomes insignificant at a large value of λ, therefore, the decrease in p_c also becomes insignificant. We may, from the above argument, speculate that there exists a limit of p_c as $\lambda\to\infty$. However, we are unable to quantitatively estimate this limit from the results we have obtained.

TABLE I. Effects of disk size ratio λ on percolation threshold and on cluster structure.

λ	p_c	D	α
1	0.550	1.874	3.649
2	0.485	1.872	3.438
3	0.437	1.879	3.308
4	0.413	1.864	3.245
5	0.400	1.861	3.104

Comparing the random packings and largest clusters in Fig. 1, we can observe that in the random packing there exist isolated clusters of small disks surrounded by the large disks, and the lower the p the more the isolated clusters. Statistics showed that at the percolation threshold p_c the largest clusters averagely contain about 56% of the total small disks. We can also observe that in the largest clusters there exist tangling disks that do not carry the current when a potential difference is applied at two opposite sides of the random packing.

As defined by Eq. (1), the percolation threshold p_c is the ratio of the area of small disks to the area of total disks. At p_c we may also examine the effect of λ on the percolating space by defining another percolation threshold p_c' as the ratio of the area of the small disks to the area covered by the disks that is

$$p_c'=\frac{\pi n_s}{4L^2}. \tag{3}$$

This definition is similar to that of the continuum percolation. Observing Eqs. (1)–(3), we have $p_c'=p_c\Phi$, here Φ is the final random packing density at p_c. Φ, p_c, and p_c' as functions of λ are shown in Fig. 5. One can observe that as λ increases p_c' also decreases, which means that, with a larger value of λ, using less small disks can generate percolating network.

To further examine the effect of λ and verify the above results, for $\lambda=2$ we studied the percolation threshold of the large disks. The area fraction of the large disks is given by

$$p=\frac{n_l\lambda^2}{n_s+n_l\lambda^2}. \tag{4}$$

Simulation results show that p_c lies between 0.650 and 0.660, and by the transformation $p_c'=p_c\Phi$ we obtain that p_c'

lies between 0.565 and 0.574. Comparing the values of p_c and p_c' of the large disks with that of the small disks $p_c = 0.485$ and $p_c' = 0.420$ one can obviously see the significant effect of the disk size ratio λ on the percolation threshold. In practice, such results may provide many benefits to the design of composites. By selecting λ one may save the valuable metal component, reduce the mass density, adjust the mechanical, electrical and thermal properties of the composites.

From the percolation thresholds p_c obtained with different system sizes, we can estimate the percolation thresholds $p_{c\infty}$ of infinite system. For the random packings of equal disks with different system sizes, see Fig. 3, we use the values of p corresponding to the percolation probabilities $G'(p) = 0.1,0.2,0.3,...,0.9$, to calculate the width Δ of the critical transition region by the equation

$$\Delta^2 = \langle p^2 \rangle - \langle p \rangle^2, \tag{5}$$

where $\langle\ \rangle$ means average. Then we can determine the correlation length exponent ν from the scale

$$\Delta \propto L^{-1/\nu}. \tag{6}$$

In the random packing, the values of L corresponding to $n = 10\,000$, 20 000, and 40 000 are 95.3, 134.7, and 190.5 respectively. From Eqs. (5) and (6), we obtain $\nu = 1.37$. It is close to the exact 2D correlation length exponent, 4/3. Two reasons make it impossible to determine ν with $\lambda > 1$. The first one is due to the small number of samples, 40 at each point of p, which will give a poor result. The second is that we fixed the system size n to 20 000, thus, at given λ, L decreases as p increases. ν is believed to be a universal parameter. Therefore, we use $\nu = 4/3$ to estimate the effect of the finite system size on the percolation threshold. It is suggested [31,35] that, with free boundary, the percolation threshold p_c based upon the crossing probability converges to $p_{c\infty}$ of infinite system according to

$$p_c - p_{c\infty} \propto L^{-1-1/\nu} = L^{-7/4}. \tag{7}$$

Note that Fig. 4 shows results with $n = 40\,000$ for $\lambda = 1$, and $n = 20\,000$ for $\lambda > 1$, thus the minimal value of L is about 170 with $\lambda = 2$. Therefore, the convergence $p_c - p_{c\infty}$ is in the order of 10^{-4}, which can be neglected as we estimated p_c to the order of 10^{-3}. Renormalization-group and some other methods estimate the convergence in a very slow way as $p_c - p_{c\infty} \propto L^{-1/\nu}$. The fast convergence is given in [35] as $p_c - p_{c\infty} \propto L^{-2-1/\nu}$ for square lattice with periodical boundary.

B. The fractal dimension

To examine the effect of λ on the cluster structure we employ the cluster radius R, which has been used by many [1,23] and is defined as

$$2R^2 = \sum_{ij} \frac{d_{ij}^2}{s^2}, \tag{8}$$

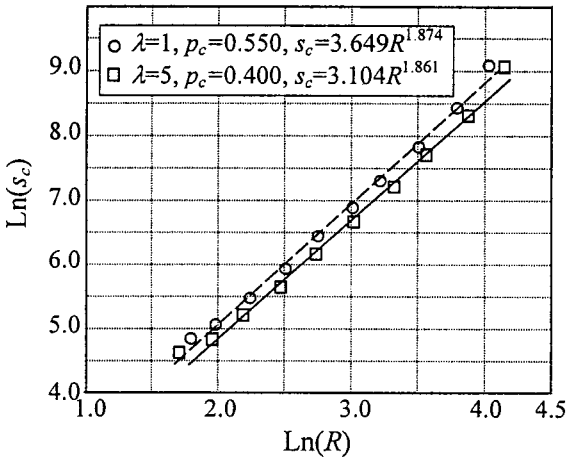

FIG. 6. Fractal dimensions of clusters at percolation thresholds.

where s is the cluster size, the number of disks belonging to the same cluster, and d_{ij} is the distance between two disks. R and L have the same dimension, which equals one. Near the percolation threshold p_c the cluster size s_c can be scaled with the cluster radius R as

$$s_c \propto R^D, \quad (p = p_c, s_c \gg 1), \tag{9}$$

where the exponent D is called the fractal dimension. Percolation theory proves that D is a universal parameter that it is independent of the packing lattices, and in the limit $L \to \infty$, $D = 91/48 = 1.896$ in 2D lattices, and D is approximately equal 2.5 in 3D lattices [1]. Lorenz, Orgzali, and Heuer indicated that this universal law is also applicable to the continuum percolation models of binary disks [23]. Thus, we may conjecture that, in the random packing of binary disks, this universal law will also be tenable. At the percolation thresholds, as listed in Table I, for each value of λ, we calculated the values of R of all the clusters. For $\lambda = 1$ and $\lambda = 5$, the symbols in Fig. 6 show the relationship between Ln(s_c) and Ln(R) both are average values in the given intervals. To determine the fractal dimension D, we applied least-square-error regression to fit the data to $s_c = \alpha R^D$ in which only the clusters $s_c > 100$ were taken into account. The values of α and D corresponding to the values of λ are also listed in Table I. For $\lambda = 3$, α and D are the averages of the values obtained with $p = 0.435$ and 0.440, and for $\lambda = 4$ they are the averages of the values obtained with $p = 0.410$ and 0.415. First we can observe that for all values of λ, the clusters have fractal dimension D in the range of 1.861–1.880, and D is independent of λ. The values of D obtained in our simulation are in good agreement with the theoretical value $D = 1.896$ of the ordered lattice percolation and with that of the continuum percolation models of binary disks [23]. This agreement supports our conjecture that, at the percolation threshold p_c, the cluster dimension D of the random packing of binary disks obeys the universal law. We may also expect that, in the limit $L \to \infty$, D would approach the theoretical value of 1.896.

Another important finding in our simulation is that, observing Table I the parameter α decreases with the increase

in λ. From the scaling equation $s_c = \alpha R^D$ we see that with the same cluster size s_c, the decrease in α results in the increase in the cluster radius R as shown in Fig. 6. This indicates that with the same size s_c, the cluster in the random packing with higher size ratio λ can span larger area. In another words, to span the same area the cluster size s_c is smaller with higher λ than that with lower λ. This observation is identical with the fact that the percolation threshold p_c decreases with the increase in λ. Figure 6 shows the trend of the divergence of the simulation values from the fitted values for small and large clusters. As indicated by the condition, Eq. (9) is not applicable to small clusters. While the finite packing area L^2 restricts the extension of the largest clusters, as shown in Fig. 1, which leads to the cluster radius R to be smaller than it should be in an infinite system.

IV. CONCLUSION

Monte Carlo study on the percolation and cluster structure of the random packing of binary disks has been reported in this paper. Results showed that the disk size ratio λ significantly influences the percolation threshold p_c of the small disks that the increase in λ leads to the decrease in p_c. For $\lambda = 1$, the packing density and the average number of the nearest neighbors in our study both lie between that of the square and triangular packings, which requires that the percolation threshold of the random packing must also lie between the percolation thresholds of the two ordered packings. Our result fulfils this requirement, which supports our conclusion about the effect of λ on p_c. Cluster structure characterization confirmed that, at percolation threshold p_c, the fractal dimension D of the clusters is independent of λ and is in good agreement with that of the classical percolation model and with the continuum percolation model. This may suggest that, as is found in classical percolation, near the percolation threshold, the physical properties of the random packing obey the universal law $\psi \propto (p - p_c)^\beta$, in which the exponent β is insensitive to the details of the microstructure of the packing. The simulation results may provide benefit in optimizing the physical properties of the composites by adjusting the compositions, such as to gain good conductivity meanwhile still retaining the high resistance to wear of the conductive ceramics. The configurations generated by this model can be used to study the hopping transport problems in amorphous solids. With simple modification, this model has been applied to 3D percolation. Further work is focusing on the identification and elimination of the tangling disks in the percolating cluster. This will allow us to build up an effective resistance network analogous to the percolating cluster.

[1] D. Stauffer and A. Aharony, *Introduction to Percolation Theory*, 2nd ed. (Taylor & Francis, London, 1994).
[2] M. Sahimi, *Applications of Percolation Theory* (Taylor & Francis, London, 1994).
[3] Z. Ball, H. M. Phillips, D. L. Callahan, and R. Sauerbrey, Phys. Rev. Lett. **73**, 2099 (1994).
[4] A. K. Gupta and A. K. Sen, Phys. Rev. B **57**, 3375 (1998).
[5] B. Hamilton, J. Jacobs, D. A. Hill, R. F. Pettifer, D. Teehan, and L. T. Canham, Nature (London) **393**, 443 (1998).
[6] K. Kato, S. Todo, K. Karada, N. Kawashima, S. Miyashita, and H. Takayama, Phys. Rev. Lett. **84**, 4204 (2000).
[7] M. Rühländer and C. M. Soukoulis, Phys. Rev. B **63**, 085103 (2001).
[8] S. Ilani, A. Yacoby, D. Mahalu, and Hadas Shtrikman, Science **292**, 1354 (2001).
[9] P. L. Leath and G. R. Reich, J. Phys. C **11**, 4017 (1978).
[10] R. M. Ziff, P. T. Cummings, and G. Stell, J. Phys. A **17**, 3009 (1984).
[11] H. F. El-Nashar, W. Wang, and H. A. Cerdeira, Phys. Rev. E **58**, 4461 (1998).
[12] L. Nurminen, A. Kuronen, and K. Kaski, Phys. Rev. B **63**, 035407 (2000).
[13] M. E. J. Newman and R. M. Ziff, Phys. Rev. Lett. **85**, 4104 (2000).
[14] R. Dobrin and P. M. Duxburn, Phys. Rev. Lett. **86**, 5076 (2001).
[15] A. Malliaris and D. T. Turner, J. Appl. Phys. **42**, 614 (1971).
[16] F. Bueche, J. Appl. Phys. **43**, 4837 (1972).
[17] R. P. Kusy, J. Appl. Phys. **48**, 5301 (1977).
[18] W. Luzny and E. Banka, Macromolecules **33**, 425 (2000).
[19] Y. Fu, M. Willander, and J. Liu, J. Electron. Mater. **30**, 866 (2001).
[20] G. van de Goor, P. Sagesser, and K. Berroth, Solid State Ionics **101**, 1163 (1997).
[21] J. Janzen, J. Appl. Phys. **52**, 2279 (1980).
[22] W. J. Kim, M. Taya, K. Yamada, and N. Kamiya, J. Appl. Phys. **83**, 2593 (1998).
[23] B. Lorenz, I. Orgzali, and H.-O. Heuer, J. Phys. A **26**, 4711 (1993).
[24] J. Quintanilla and S. Torquato, Phys. Rev. E **54**, 5331 (1996).
[25] J. Quintanilla, S. Torquato, and R. M. Ziff, J. Phys. A **33**, L399 (2000).
[26] J. Asikainen and T. Ala-Nissila, Phys. Rev. E **61**, 5002 (2000).
[27] D. He, N. N. Ekere, and L. Cai, Phys. Rev. E **60**, 7098 (1999).
[28] J. M. Berryman, Phys. Rev. A **27**, 1053 (1983).
[29] B. D. Lubachevsky, F. H. Stillinger, and E. N. Pinson, J. Stat. Phys. **64**, 501 (1991).
[30] J. L. Cardy, J. Phys. A **25**, L201 (1992).
[31] R. M. Ziff, Phys. Rev. Lett. **69**, 2670 (1992).
[32] C. Hu, C. Lin, and J. Chen, Phys. Rev. Lett. **75**, 193 (1995).
[33] S. B. Lee and S. Torquato, Phys. Rev. A **41**, 5338 (1990).
[34] R. R. Zallen, *The Physics of Amorphous Solids* (Wiley, New York, 1998).
[35] M. E. J. Newman and R. M. Ziff, Phys. Rev. E **64**, 016706 (2001).